

CENTRIFUGAL PUMPING IN THE EQUIFORCE SPIRAL MICROCHANNEL

Xing Yue (Larry) Peng¹ and *Paul CH Li²

¹Department of Biology, Xiamen University, Xiamen, Fujian, China 361005

²Department of Chemistry, Simon Fraser University, Burnaby, British Columbia, Canada V5A1S6

ABSTRACT

In order to create a multi-sample-multi-probe DNA microarray on a circular disk (CD), we have designed numerous equiforce spiral microchannels on it. Hydrodynamic DNA sample hybridizations occurred in these channels when the samples were delivered by centrifugal pumping. The main goal of the use of the equiforce microchannel is to ensure a constant liquid flow velocity as the sample is filled through an empty spiral channel. Nevertheless, the design of the equiforce spiral channel has not been reported. In this work, the mathematical equation of the spiral curve and its physical basis for the equiforce condition are reported for the first time, and the constant flow velocity has been proven by a detailed image analysis of the liquid front advancing inside the microchannel. The sensitivity tests of various design parameters on the flow velocity in the spiral channel were revealed in detail.

Keywords: Microfluidic device, centrifugal pumping, equiforce spiral channel, DNA microarray.

INTRODUCTION

The microarray method has been widely used for many biotechnological applications, such as DNA-based pathogen detection (Campas and Katakis, 2004). We have developed a full microfluidic method in which no spotting is needed and multiple samples can be applied (Peng *et al.*, 2007; Wang *et al.*, 2008). In this method, both the microarray creation and its application to DNA hybridization are conducted by microfluidic operations on a circular disk (CD). The microfluidic microarray method has been applied for hybridization of complementary oligonucleotides (Peng *et al.*, 2007) and PCR products (Wang *et al.*, 2008). In these reports, after a line microarray is printed using radial channels (Fig. 1A), the test chip is assembled with a spiral channel plate (Fig. 1B). When the assembly is spun, an along-channel component of the pseudo centrifugal force is developed along the spiral channel. This component force results in the liquid flow in the spiral channels, which intersect with the line microarray created in the previous step. Thus, we benefit from the use of centrifugal pumping for convenient DNA sample delivery and hydrodynamic hybridization inside the equiforce spiral microchannels to form a spot microarray.

Since the centrifugal force tends to increase with the radius, the velocity of the sample solution will increase as it flows from the inlet reservoir near the centre to the outlet reservoir near the CD rim. This increasing flow velocity is undesirable because the residence time for hybridization becomes shorter and shorter as the liquid flows toward the outlet reservoir. In order to achieve uniform hybridization results, it is essential to ensure a constant flow velocity of DNA samples in the spiral

channels, especially when the small sample volume (e.g. 1 μ l) employed is a significant portion of the total sample volume during channel filling. Therefore, we should design a special spiral channel (Fig. 2A), which maintains a constant along-channel component centrifugal force ($C \cos \alpha$) over the whole channel, regardless of the locations near the centre or the rim of the CD.

THEORY

On the rotating frame of reference of a spinning CD, the reaction force P that exerts perpendicularly from the channel wall to a short column of liquid is balanced by the pseudo cross-channel centrifugal force component $C \sin \alpha$ (Fig. 2B). However, there is no reaction force along the channel, and so a pseudo along-channel component of the centrifugal force $C \cos \alpha$ causes the liquid to move along the spiral channel. When this along-channel force $C \cos \alpha$ is balanced by the liquid resistance force R that includes the viscous drag force and the surface tension of the advancing liquid front, the flow attains a constant terminal velocity.

Since C increases with the radius, as depicted by the increasing magnitude of the radial vectors in figure 2B, a constant terminal velocity of the liquid will not be attained. This would be the case if we used a simple spiral channel, such as the equiangular spiral in which the spiral curve makes a constant angle α with the radius. However, in our specially designed spiral, we have manipulated the angle α in order to maintain a constant value of the along-channel force (i.e. equiforce) anywhere along the channel. We explain this equiforce concept using a gravity analogy in figure 3, in which G represents the gravitational force in one region, and G' represents a higher force in another region (Fig. 3C). Figure 3A shows an increase of the along-slope gravitational force from $G \cos \alpha$ to $G' \cos \alpha$

*Corresponding author email : paulli@sfu.ca

because G increases to G' . But if the angle α increases to α' too (Fig. 3B), the along-slope force can be adjusted to equal its original value (i.e. $G \cos \alpha = G' \cos \alpha'$).

Therefore, the design of the spiral curve is to increase the angle α , or reduce $\cos \alpha$, to compensate for the increasing centrifugal force. In the case of a spinning CD, the along-channel acceleration (a_α) is given by

$$a_\alpha = \omega^2 r \cos \alpha \quad (1)$$

where α is the angular velocity, r is the radius, and α is the angle that the spiral curve makes with the radius (see Fig. 2A).

At the initial position of the spiral channel, $r = r_0$ and $\alpha = \alpha_0$, then we have

$$a_{\alpha_0} = \omega^2 r_0 \cos \alpha_0 \quad (2)$$

To maintain a constant along-channel force and acceleration over the entire spiral channel, we should have

$$\begin{aligned} a_{\alpha_0} &= a_\alpha \\ \text{or } r_0 \cos \alpha_0 &= r \cos \alpha \end{aligned} \quad (3)$$

From Fig. 2A, we have the following equation to describe an infinitesimal segment of the equiforce spiral curve,

$$\frac{rd\beta}{dr} = \tan \alpha = \frac{\sqrt{1 - \cos^2 \alpha}}{\cos \alpha} \quad (4)$$

where the center of the CD is also the center of the polar coordinates, and β and r are the angle and radius of the polar coordinates, respectively.

After integration of equation 4 (see appendix A), we obtain a function that describes the equiforce spiral curve,

$$\begin{aligned} \beta - \beta_0 &= \sqrt{\left(\frac{r}{r_0 \cos \alpha_0}\right)^2 - 1} - \\ & \text{ArcTan} \sqrt{\left(\frac{r}{r_0 \cos \alpha_0}\right)^2 - 1} - \text{Tan} \alpha_0 + \alpha_0 \end{aligned} \quad (5)$$

MATERIALS AND METHODS

The microchannel plates and glass test chip

The design and fabrication of the channel plates have been previously reported (Peng *et al.*, 2007). Briefly, the channel pattern is created by Visual Basic. This pattern was used to fabricate the polydimethylsiloxane (PDMS)

channel plate of 92 mm in diameter. The channel width and channel depth were 60 μm and 20 μm , respectively. The inlet reservoirs were designed in a staggered fashion to make sure the reservoirs are sufficiently far apart for efficient sample application. The glass test chip were obtained from Precision Glass & Optics. They were 4" in diameter with a 0.6" centre hole.

Flow visualization in the spiral channels

The liquid flow in the spiral channel was visualized using a solution containing a blue food dye (Scott-Bathgate, Vancouver, BC). The microchannels were illuminated by a stroboscope light (Monarch, Nova-Strobe DA Plus 115) at the same frequency as the rotation speed which was 2500 rpm. The position of the liquid front was recorded by a video camera (SONY DCR-TRV260) equipped with a 4X lens.

To assist in the position measurement of the advancing liquid front, numerous radial lines were drawn on a piece of paper that was put under the glass chip. Each image frame of the video clip was studied and measured to determine the times and positions of the liquid fronts. Therefore, the flow velocities of the advancing liquid front meniscus during the filling of the spiral microchannels were determined.

RESULTS AND DISCUSSION

The liquid movement in the spiral channels was first examined using the blue-dyed solutions. As shown in figure 4A, it was observed that the solution left the inlet solution reservoir and flowed through the spiral channel. Figure 4B shows various dimensions and forces near the inlet reservoir of the spiral channel.

The information of distance and transit time of the advancing liquid front were determined in each spiral channel and displayed graphically. Figure 5A shows the overlay of 96 traces of the transit time plotted against the liquid front position. The liquid front velocity is given by the reciprocal of the slope. In each trace, it is observed that the liquid front reaches the constant slope (or constant velocity) after traveling for 50 mm, albeit the values are different in different channels, possibly due to different channel conditions. The slower initial liquid front velocity (or greater slope) was attributed to the surface tension barrier resistance that the liquid encountered when it entered the microchannel. Moreover, it is seen that the constant velocities in all channels are within a range of 5 ± 1 mm/s. Note that the velocity in each spiral channel is constant within a much narrower range.

To model the liquid flow speed in the spiral microchannel, a schematic diagram near the inlet reservoir of the channel has been shown in figure 4B. At the end of the short straight channel (L_0), the channel

changes its direction (i.e. at an angle α_0 to the radius) along the spiral channel. The liquid in the reservoir is shown to be continually filled into the empty spiral microchannel. In the modeling work, one usually uses the Navier-Stokes equation, which is based on conservation of momentum and is formulated by a balance of the body force (centrifugal force) and surface force (viscous drag force) to the liquid pressure field. The line force (surface tension effect) comes into play as a boundary condition. Nevertheless, under the condition of a constant body force anywhere inside the equiforce spiral channel, we simplify the modeling work by directly using just the force balance in a 1-dimensional approximation.

In this simplified model, the body force (F) is considered as a linear accumulation of the constant centrifugal force of infinitesimal liquid elements within the spiral channel. Therefore, F increases with the column length L as follows.

$$F = \rho X L a_{\alpha_0} \quad (6)$$

where ρ is the liquid density; X is the cross-section area; L is given by equation A8 (see appendix A).

Using equation 2, we have

$$F = \rho X L \omega^2 r_0 \cos \alpha_0 = k_1 L \quad (7)$$

$$\text{where } k_1 = \rho X \omega^2 r_0 \cos \alpha_0 \quad (8)$$

Similarly, the body force (F_0) due to the liquid in the initial radial straight channel section is considered to a constant, and is given by

$$F_0 = k_1 L_0 \quad (9)$$

Next, we consider the surface force (F_2) which is also a linear accumulation of the viscous drag force of infinitesimal liquid elements. F_2 which increases linearly as the contact area of the liquid column becomes increasingly larger is given by

$$F_2 = \mu A \frac{du}{dy} \quad (10)$$

where μ is the viscosity coefficient; du/dy is the velocity gradient across the channel width; A is the contact area of the liquid column layer, which increases linearly as the liquid filling length ($L + L_0$).

The velocity gradient du/dy is proportional to the maximum velocity ($u = dL/dt$) at the centre of the channel. In fact, it was the position of the centre of the liquid front that was measured as L in the experiments. Then we lump all constants into k_2 to give

$$F_2 = k_2 (L + L_0) \frac{dL}{dt} \quad (11)$$

At the liquid front, the line force (S), which is the surface tension at the liquid front exists, is considered to be constant. For a constant liquid flow velocity, the forward driving forces (F_0 and F) must be balanced by the backward forces (F_2 and S) as follows

$$F + F_0 = F_2 + S \quad (12)$$

Combining equations 7, 11 and 12, we have

$$k_1 L + b = k_2 (L + L_0) \frac{dL}{dt} \quad (13)$$

$$\text{where } b = S - F_0 \quad (14)$$

For integration, equation 13 is transformed to give

$$dt = \frac{k_2 (L + L_0)}{k_1 L + b} dL \quad (15)$$

After integration, we have

$$t = k_2 \left(\frac{L}{k_1} + \frac{k_1 L_0 - b}{k_1^2} \ln(k_1 L + b) \right) + D \quad (16)$$

where D is the integration constant. By using equation 14 and lump all constants not associated with L into D' , we have a flow equation relating the transit time (t) and the filling column length (L):

$$t = \frac{k_2}{k_1} L + \frac{k_2 (k_1 L_0 + S - F_0)}{k_1^2} \ln \left(L - \frac{S - F_0}{k_1} \right) + D' \quad (17)$$

The plot of transit time versus distance for one spiral channel is shown in Figure 5C. Using regression analysis, the data was fitted to equation 17 to give $t = 0.136L + 3.599 \log(L - 0.476) + 0.272$. The agreement ($R = 0.9996$) between the experimental data (circles) and the fitted curve is excellent, thus verifying the theoretical model.

Subsequently, various sensitivity tests were performed in order to determine the optimal conditions to reach a constant flow velocity even during the initial section of the spiral channel. For instance, when the $S - F_0$ was decreased (down to 1/32 of the original value), the linearity of the curve became better (Fig. 6A), indicating that the constant flow velocity was attained over most parts of the spiral channel. In the case of modifying S, the flow velocity (as given by the reciprocal of the slope) did not change greatly, indicating that there was no sacrifice in the flow time.

When the viscosity (μ) was reduced (down to 1/32 of the original value), the linearity of the curve also became better (Fig. 6B), indicating the achievement of constant flow velocity in most parts of the spiral channel. However, the flow velocities became increasingly higher, as evident from the reduction in slopes. This would require the reduction in the spinning speed of the CD in order to maintain the same flow velocity and reaction residence time. Furthermore, when the driving force F was increased, the linearity of the curve became better (Fig. 6C), but the flow velocities became higher too.

Based on these sensitivity tests, we identify some ways to expand the range of constant flow velocity. For instance, we can spin the CD faster or design a spiral with a larger α_0 . In both cases, a stronger centrifugal force can be

obtained to overcome the surface tension barrier. Nevertheless, this stronger centrifugal force generates a higher flow velocity, and so there is insufficient time for the hybridization reaction to complete for the DNA microarray work. The best way is to use a surfactant to decrease the surface tension barrier. This method does not result in any increase in the flow velocity (Fig. 6A), and the range of constant flow velocity can be expanded to nearly the whole channel.

CONCLUSIONS

Flow velocity in a spiral microchannel on CD was properly controlled to be constant based on the equiforce spiral formulation. In this case, the centrifugal force is equal at every location along the spiral microchannel. Various sensitivity tests have been performed on the simulated distance-time curves, leading to some useful design and operational parameters. This equiforce condition has resulted in effective hybridizations as reported in our previous work.

ACKNOWLEDGEMENT

We thank Natural Sciences and Engineering Research Council of Canada for a Discovery Grant. XY Peng thanks National Science Foundation of China.

Appendix A: Mathematical derivation of the equiforce spiral curve

Equation 4 has been given to describe an infinitesimal segment of the equiforce spiral curve,

$$\frac{rd\beta}{dr} = \tan \alpha = \frac{\sqrt{1 - \cos^2 \alpha}}{\cos \alpha} \tag{4}$$

where the center of the CD is also the center of the polar coordinates, and β is the angle and r is the radius of the polar coordinates, see Fig 2.

From equation 1 shown previously, we substitute k for

$$\frac{a_\alpha}{\omega^2}$$

. Then we have

$$k = \frac{a_\alpha}{\omega^2} = r \cos \alpha \tag{A1}$$

Combining equation A1 with equation 3, we have

$$k = r_0 \cos \alpha_0 \tag{A2}$$

Combining equation 4 and equation A1, we have

$$\frac{rd\beta}{dr} = \frac{\sqrt{1 - \frac{k^2}{r^2}}}{\frac{k}{r}} \tag{A3}$$

Separating the variables, and integrating with the limits from β_0 to β , and from r_0 to r as follows,

$$\int_{\beta_0}^{\beta} d\beta = \int_{r_0}^r \frac{\sqrt{1 - \frac{r^2}{k^2}} - 1}{r} dr \tag{A4}$$

After integration, we have

$$\beta - \beta_0 = \sqrt{\left(\frac{r}{k}\right)^2 - 1} - \text{ArcTan}\sqrt{\left(\frac{r}{k}\right)^2 - 1} - \sqrt{\left(\frac{r_0}{k}\right)^2 - 1} + \text{ArcTan}\sqrt{\left(\frac{r_0}{k}\right)^2 - 1} \tag{A5}$$

After using equation A2 to replace k , we obtain a function that describes the equiforce spiral curve based on the polar coordinates r and β ,

$$\beta - \beta_0 = \sqrt{\left(\frac{r}{r_0 \cos \alpha_0}\right)^2 - 1} - \text{ArcTan}\sqrt{\left(\frac{r}{r_0 \cos \alpha_0}\right)^2 - 1} - \text{Tan} \alpha_0 + \alpha_0 \tag{5}$$

The value of β_0 in equation 5 is computed by numerical iteration (Ypma, 1995) using the known value of r_0 and r_1 , and the condition that $r = r_1$ leads to $\beta = \beta_0 + 2\pi$. In our design, α_0 is computed to be 1.4517 radians.

To assist in the numerical iteration to compute α_0 , the following partial differential equation is obtained from equation 5 by differentiating it with respect to α_0 ,

$$\frac{\partial(\beta - \beta_0)}{\partial \alpha_0} = 1 - \text{Sec}^2 \alpha_0 - \frac{\text{Tan} \alpha_0 - \left(\frac{r}{r_0}\right)^2 \text{Sec}^2 \alpha_0 \text{Tan} \alpha_0}{\sqrt{\left(\frac{r}{r_0}\right)^2 \text{Sec}^2 \alpha_0 - 1}} \tag{A6}$$

With a computed α_0 we can plot the equiforce spiral curve using equation 5.

In order to plot the spiral curve, we have to obtain the β value at each value of r , using numerical iteration. To assist in this operation, we use another partial differential equation obtained from equation 5 by differentiating it with respect to r ,

$$\frac{\partial(\beta - \beta_0)}{\partial r} = \sqrt{\frac{1}{r_0^2 \text{Cos}^2 \alpha_0} - \frac{1}{r^2}} \tag{A7}$$

In addition, the following equation allow us to calculate the length of liquid column, L , in the spiral microchannel.

$$L = \frac{1}{2r_0 \text{Cos} \alpha_0} (r^2 - r_0^2) \tag{A8}$$

With $\alpha_0 = 1.4517$ radians, $r_0 = 24$ mm and $r_1 = 42$ mm, L is computed to be 208 mm.

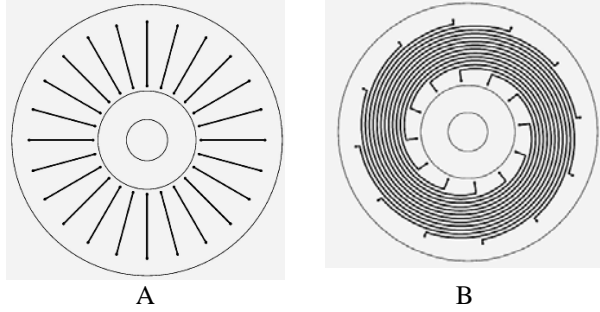


Fig. 1. Schematics of the microfluidic microarray method. (A) Channel plate 1 consists of 24 radial microchannels for DNA probes to fill and to be immobilized as probe lines. (B) Channel plate 2 consists of 12 spiral microchannels in which DNA samples would flow and hybridize to the probe lines. Although these channel numbers are 12 or 14 for clarity, the actual number of channels fabricated on the PDMS chip are both 96.

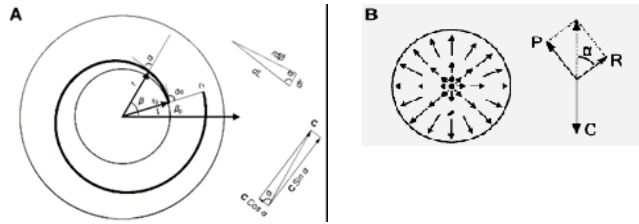


Fig. 2. (A) The design of the equiforce spiral channel depicted with the polar coordinates of r and β . The spiral curve starts at r_0 and β_0 at an angle of α_0 that the spiral curve makes with the radius. The spiral curve ends at r_1 . An infinitesimal section of the curve is given on the top right inset, showing the angular relation between $r d\beta$ and dr . (B) The force field on a spinning CD. In a rotating frame of reference, the force relationship is depicted on the right. The reaction force from the channel wall (P) and the resistance force along the channel (R) are balanced by the pseudo centrifugal force (C).

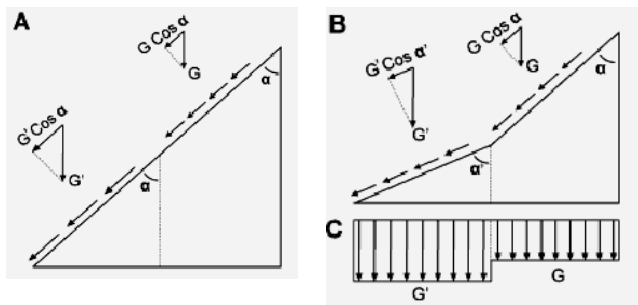


Fig. 3. The gravity analogy for the equiforce concept. (A) On a constant slope, if the gravity increases from G to G' , the along-slope force increases from $G \cos \alpha$ to $G' \cos \alpha$. (B) On a changing slope, if the angle that the slope makes with the vertical is increased from α to α' , the along-slope forces can be adjusted to remain the same (i.e. $G \cos \alpha = G' \cos \alpha'$). (C) The gravitational force increases from G to G' .

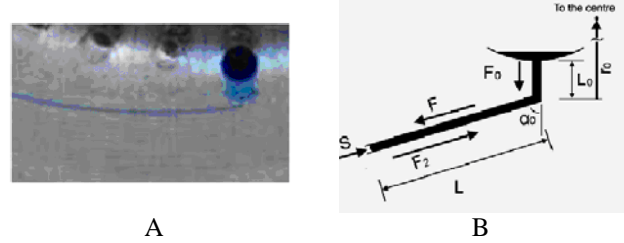


Fig. 4. Characterization of liquid flow in the equiforce spiral channel. (A) The liquid (dyed solutions) was successfully filled into one spiral microchannel during spinning or rotation of the chip. (B) The schematic diagram of a spiral channel near the inlet reservoir, showing the model parameters. L_0 is the length of the short straight channel connecting the inlet reservoir to the spiral channel. The junction of the straight and spiral channels makes an angle of α_0 , and is r_0 away from the CD centre. The length of the filling liquid column in the equiforce spiral channel is L . The along-channel centrifugal force components in the constant straight portion and variable radial portion are given by F and F_0 , respectively. The liquid viscous drag force is given by F_2 . The surface tension at the liquid front meniscus is given by S .

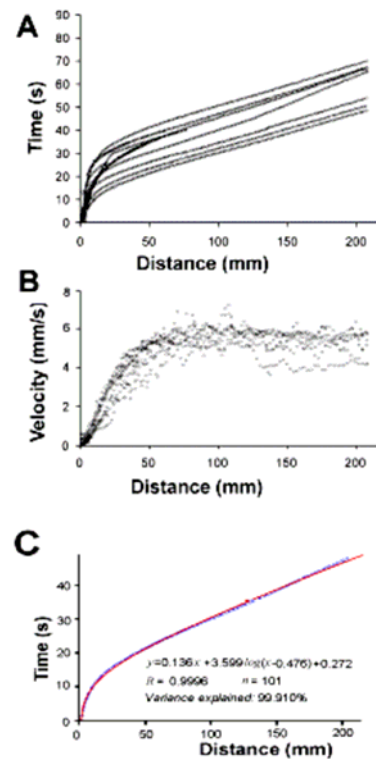


Fig. 5. Flow dynamics in the equiforce spiral channel. (A) The transit times of the flow in 96 spiral microchannels were plotted against distance. (B) The velocities of the flow as calculated from the slopes of all 96 traces in (A). (C) Curving fitting of the experimental data in one trace (circles) to the theoretical model (line), resulting in $R = 0.9996$.

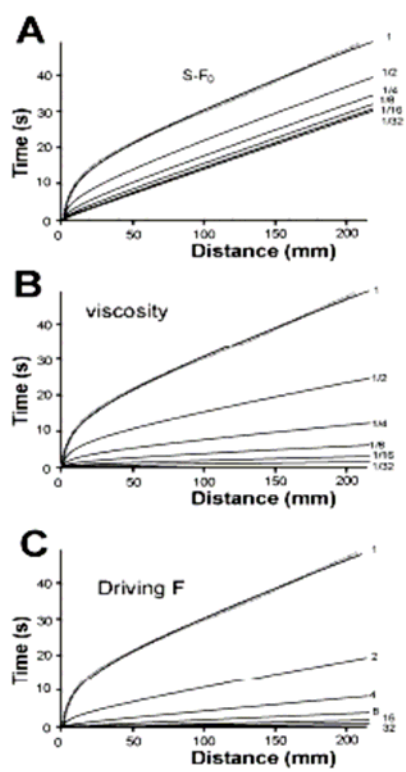


Fig. 6. Sensitivity tests for the model. (A) Sensitivity test of $S-F_0$ (1/2, 1/4, 1/8, 1/16 and 1/32 of the original value). (B) Sensitivity test of viscosity (1/2, 1/4, 1/8, 1/16 and 1/32 of the original value). (C) Sensitivity test of F (2, 4, 8, 16, 32 time of the original value).

REFERENCES

- Campas, M. and Katakis, I. 2004. DNA Biochip Arraying, Detection and Amplification Strategies. *Trends Anal. Chem.* 23: 49-62.
- Peng, XY., Li, PCH., Wang L., Yu, HZ., Parameswaran, AM. and Chou, WL. 2007. Spiral Microchannels on a CD for DNA Hybridizations. *Sens. Actuators B.* 128: 64-69.
- Wang, L., Li, PCH., Yu, HZ. and Parameswaran, A.M. 2008. Fungal Pathogenic Nucleic Acid Detection Achieved with a Microfluidic Microarray Device. *Anal. Chim. Acta.* 610: 97-104.
- Ypma, TJ. 1995. Historical development of the Newton-Raphson method, *SIAM Review* 37: 531-551.